

A universal minimal mass scale for present-day central black holes

Tal Alexander* and Ben Bar-Or†

Intermediate-mass black holes (IMBHs) of mass $M_\bullet \approx 10^2\text{--}10^5$ solar masses, M_\odot , are the long-sought missing link¹ between stellar black holes, born of supernovae², and massive black holes³, tied to galaxy evolution by the empirical M_\bullet/σ_\star correlation^{4,5}. We show that low-mass black hole seeds that accrete stars from locally dense environments in galaxies following a universal M_\bullet/σ_\star relation^{6,7} grow over the age of the Universe to be above $\mathcal{M}_0 \approx 3 \times 10^5 M_\odot$ (5% lower limit), independent of the unknown seed masses and formation processes. The mass \mathcal{M}_0 depends weakly on the uncertain formation redshift, and sets a universal minimal mass scale for present-day black holes. This can explain why no IMBHs have yet been found³, and it implies that present-day galaxies with $\sigma_\star < \mathcal{S}_0 \approx 40 \text{ km s}^{-1}$ lack a central black hole, or formed it only recently. A dearth of IMBHs at low redshifts has observable implications for tidal disruptions⁸ and gravitational wave mergers⁹.

The early stages of massive black hole growth are poorly understood¹⁰. High-luminosity active galactic nuclei at very high redshift¹¹ z further imply rapid growth soon after the Big Bang. Suggested formation mechanisms typically rely on the extreme conditions found in the early Universe (very low metallicity, very high gas or star density). It is therefore plausible that these black hole seeds were formed in dense environments, at least a Hubble time ago ($z > 1.8$ for a look-back time of $t_H = 10 \text{ Gyr}$)¹².

The relation $M_\bullet = M_s(\sigma_\star/\sigma_s)^\beta$ between black hole mass, M_\bullet , and stellar velocity dispersion, σ_\star , that is observed in the local Universe over more than about three decades in massive black hole mass, correlates M_\bullet and σ_\star on scales that are well outside the massive black hole's radius of dynamical influence³, $r_h \approx GM_\bullet/\sigma_\star^2$. Recent analyses of large heterogeneous galaxy samples find that a universal M_\bullet/σ_\star relation holds for all galaxy types^{6,7}, although the scope of this relation and its evolution with redshift remain controversial¹³. Here we adopt the empirical fit⁷ $\log_{10}(M_\bullet/M_\odot) = 8.32 \pm 0.04 + \delta_\epsilon + (5.35 \pm 0.23) \log_{10}(\sigma_\star/200 \text{ km s}^{-1})$, where $\delta_\epsilon = 0.49 \pm 0.03$ is the root mean square of the intrinsic scatter. We assume that this universal M_\bullet/σ_\star holds at all redshifts¹⁴, and that the black hole seeds grow in a locally (within a few r_h) dense stellar environment. By fixing r_h , the M_\bullet/σ_\star relation then imposes tight connections between the black hole and the dynamical properties of its stellar surroundings¹⁵, and specifically the rate at which it consumes stars (see Methods section).

A central black hole grows by (1) the accretion of stars, compact remnants and dark matter particles that are deflected toward it on nearly radial orbits, and either fall whole through the event horizon or are tidally disrupted outside it, and then accreted; (2) viscosity-driven accretion of interstellar gas; and (3) mergers with other black holes. Of these growth channels, only the accretion of stars must follow from the existence of a central black hole in a stellar system. Moreover, the tidal disruption event

(TDE) rate in steady-state can be estimated from first principles, for given boundary conditions at r_h (ref. ¹⁶).

It has been noted that typical steady-state TDE rates, Γ , around 10^{-4} yr^{-1} (Fig. 1), imply by simple dimensional analysis that massive black holes (MBHs) with low mass, $\lesssim 10^7 M_\odot$, may acquire a substantial fraction of their mass from TDEs over the Hubble time t_H , or equivalently, that linear growth by TDEs has a typical mass scale^{17–19}, $M_\bullet^{\text{TDE}} \sim M_\star \Gamma t_H \sim 10^6 M_\bullet$ (however, the growth equation is generally nonlinear, and therefore M_\bullet^{TDE} can significantly mis-estimate $M_\bullet(t_H)$; see Methods section). Previous studies have usually focused on the rates and prospects of TDE detection, and not on black hole growth. Although it was recently argued that M_\bullet^{TDE} arises as a minimal black hole mass in a specific formation scenario¹⁹, the commonly held assumption remains that IMBHs with $M_\bullet \ll M_\bullet^{\text{TDE}}$ do exist, and that this must constrain formation scenarios, or set an upper bound on the efficiency of TDE accretion, rather than a lower bound on IMBH masses¹⁸.

Here, we argue that IMBHs are transient objects, which no longer exist in the present-day Universe. We derive a universal lower bound on the present-day mass scale of central black holes, \mathcal{M}_0 , that follows directly from the universal M_\bullet/σ_\star relation, and is independent of the unknown seed masses and their formation processes. We use the M_\bullet/σ_\star relation to set the boundary conditions, and show that the nonlinear growth equation for black holes can be bounded from below by a simple inequality that includes only growth by TDEs. We translate the intrinsic scatter in the M_\bullet/σ_\star relation to a probability distribution for the lower bounds \mathcal{M}_0 and \mathcal{S}_0 , and show that \mathcal{M}_0 lies just below the lightest MBHs yet discovered³, $\mathcal{M}_0 \lesssim \min(M_\bullet^{\text{obs}}) \sim 10^6 M_\odot$.

Stars around a central black hole are constantly scattered in angular momentum to nearly radial orbits below a critical (“loss-cone”) value, $j_{lc} = \sqrt{1 - e^2}$ (e is the orbital eccentricity), which approach the black hole closer than the tidal disruption radius, $r_t \simeq (M_\bullet/M_\star)^{1/3} R_\star$ (M_\star and R_\star are the stellar mass and radius), where they are destroyed. Main sequence stars are disrupted outside an IMBH's event horizon, and a fraction f_a of about 1/4 to 1/2 of their mass is ultimately accreted by the black hole²⁰. The TDE rate depends on the number of stars near the black hole and on the competition between the two-body relaxation time T_R (equation (12)) and the orbital time in supplying and draining loss-cone orbits. The integrated contribution in steady-state from all radii is a function of M_\bullet and of the boundary conditions at r_h , fixed by σ_\star . The TDE rate is well-approximated by a power-law $\Gamma \simeq \Gamma_\star (M_\bullet/M_\star)^b$, whose index b is a function of the M_\bullet/σ_\star index β , and changes across a critical mass scale $M_c \sim 10^6 M_\odot$ (Fig. 1; see Methods section). The index $b \ll 1$ for the empirical range $4 \lesssim \beta < 6$ (refs ^{3,13}).

Let us assume that a black hole seed forms with an initial mass M_i large enough to dominate its radius of influence, in a central stellar system that is massive enough to allow it to grow: that is, $M_{\text{sys}} \gg r_h^3 M_\star n_\star(r_h) > M_\bullet \gg M_\star$ at all times (n_\star is the

*Department of Particle Physics & Astrophysics, Weizmann Institute of Science, Rehovot 76100, Israel.

†Institute for Advanced Study, Einstein Drive, Princeton, NJ 08540, USA

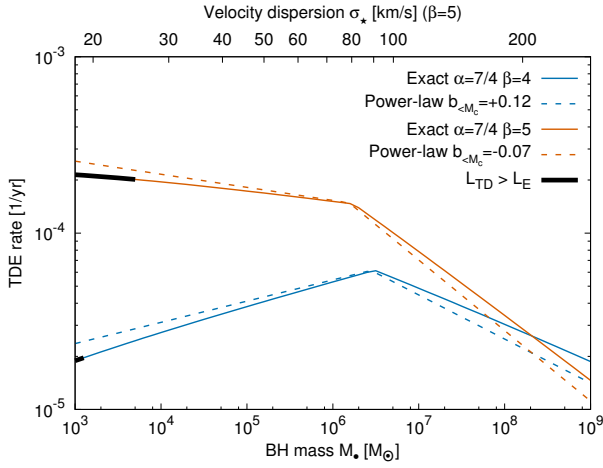


Figure 1 | Plunge rates as function of the black hole mass M_* . Rates (solid lines, see Methods section) are plotted for $M_* = 1 M_\odot$, $R_* = 1 R_\odot$, $f_a = 3/8$, $\alpha = 7/4$, and $\beta = 4, 5$, normalized to the empirical M_\bullet/σ_* mass parameter $M_s = 2.1 \times 10^8 M_\odot$ ⁷. The corresponding velocity dispersion σ_* is displayed for a $\beta = 5 M_\bullet/\sigma_*$ relation. The rates are well-approximated by power-laws (dashed lines, equation (4)). Radiation back-reaction above the Eddington limit L_E by the mean accretion luminosity $L_{TD} = \eta f_a M_* c^2 \Gamma$ ($\eta = 0.1$ assumed for the radiative efficiency) is only relevant for the lowest black hole masses, where it may slow down the initial black hole growth.

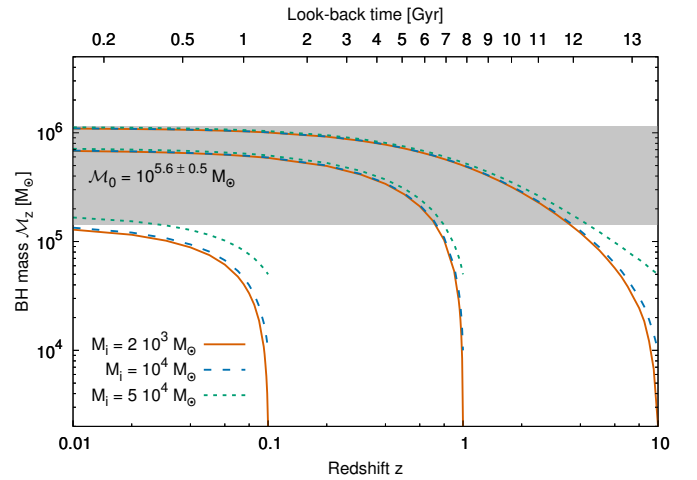


Figure 2 | Cosmological growth of the minimal black hole mass \mathcal{M}_z as function of redshift. The evolution of the minimal black hole mass (equation (10)) is plotted for several values of the black hole seed mass M_i at different formation redshifts z_i (look-back times¹² t_i), assuming the empirical M_\bullet/σ_* relation⁷ without scatter, an $\alpha = 7/4$ cusp of Solar type stars and an accreted mass fraction $f_a = 3/8$. The convergence to evolution that is independent of initial mass is rapid in redshift. The earlier the formation, the higher is \mathcal{M}_0 . The range $z_i = 0.1 - 10$ translates to a lower mass limit on present-day MBHs $\mathcal{M}_0 \sim 10^{(5.6 \pm 0.5)} M_\odot$ (gray band).

stellar density). Consider first the case where the black hole grows only by accreting stars. The black hole growth equation is

$$\dot{M}_\bullet = f_a M_* \Gamma_* (M_\bullet/M_*)^b \equiv \dot{M}_\bullet^*, \quad M_\bullet(0) = M_i. \quad (1)$$

The solution for $b < 1$ in the $t \gg t_\infty = (M_i/M_*)^{1-b}/(|1-b|f_a\Gamma_*)$ limit (equation (9)), $M_\bullet(t) \simeq [(1-b)f_a\Gamma_*t]^{1/(1-b)} M_* \equiv M_\bullet^*(t)$, is independent of M_i . Because $t_\infty \ll t_H$ for $M_i \lesssim 10^5 M_\odot$, all seeds reach the same mass scale after $\mathcal{O}(t_H)$ (Fig. 2).

Consider next a realistic black hole that grows also by gas accretion and/or mergers, $\dot{M}_\bullet = \dot{M}_\bullet^* + \dot{M}_\bullet^+$, where $\dot{M}_\bullet^+ \geq 0$ is the accretion rate by the non-stellar channels. The full growth equation is

$$\dot{M}_\bullet = \dot{M}_\bullet^* + \dot{M}_\bullet^+ \geq f_a M_* \Gamma_* (M_\bullet/M_*)^b, \quad M_\bullet(0) = M_i. \quad (2)$$

The solution $M_\bullet^*(t)$ of the stars-only growth (equation (1)) then provides a lower limit on the actual mass $M_\bullet(t)$ of the growing black hole. Note that M_\bullet^* is not necessarily a lower limit on the actual stellar mass contribution M^* to M_\bullet : $M_\bullet^* \leq M^* \leq M_\bullet$ for $b \geq 0$, but $M^* < M_\bullet^* \leq M_\bullet$ for $b < 0$. The universal minimal mass scale of a central black hole at t_H , and the corresponding minimal velocity dispersion scale are then

$$\mathcal{M}_0 = M_\bullet^*(t_H) = [(1-b)f_a\Gamma_*t_H]^{1/(1-b)} M_*, \quad \mathcal{S}_0 = (\mathcal{M}_0/M_s)^{1/\beta} \sigma_s, \quad (3)$$

with the index b for the $M_\bullet < M_c$ branch of equation (6). This implies that galaxies with $\sigma_* < \mathcal{S}_0$ do not have a central black hole, or have formed it only recently, for otherwise the coevolution of the black hole and nucleus over t_H would have driven σ_* to a much larger present-day value.

Assuming the universal M_\bullet/σ_* relation and Solar type stars, the range in \mathcal{M}_0 values is due to the variety and uncertainty in

the properties of galactic nuclei and of tidal disruption, and to the intrinsic scatter in the relation. \mathcal{M}_0 increases with the index α of the stellar cusp ($n_* \propto r^{-\alpha}$) inside r_h , and with the accreted mass fraction f_a , from $10^5 M_\odot$ for the shallowest possible cusp of unbound stars ($\alpha = 1/2$, $f_a = 1/4$) to $10^6 M_\odot$ for a steep isothermal cusp ($\alpha = 2$, $f_a = 1/2$). $\mathcal{M}_0 \simeq 10^6 M_\odot$ for the parameters adopted here: a dynamically relaxed cusp²¹ where $\alpha = 7/4$, and an accreted mass fraction $f_a = 3/8$.

The scatter around the M_\bullet/σ_* relation likely reflects intrinsic physical differences between galaxies beyond the measurement errors on the M_\bullet/σ_* parameters⁷. This induces roughly Gaussian probability distributions for \mathcal{M}_0 and \mathcal{S}_0 : $\mathcal{M}_0 = (1.1 \pm 0.8) \times 10^6 M_\odot$ and $\mathcal{S}_0 = 79 \pm 35 \text{ km s}^{-1}$ (1σ). The lowest- σ_* galaxies known to harbor active galactic nuclei²² (and hence black holes, with estimated masses $10^5 \lesssim M_\bullet \lesssim 10^6 M_\odot$), have $\sigma_* \sim 30 - 40 \text{ km s}^{-1}$. This corresponds to the 5% lower limits $\mathcal{S}_0 \lesssim 40 \text{ km s}^{-1}$ and $\mathcal{M}_0 \lesssim 3 \times 10^5 M_\odot$, which we adopt here as representative lower limits. Lighter black holes are much rarer yet: e.g. $M_\bullet \leq 10^4 M_\odot$ is below the 0.0001% limit.

The agreement $\mathcal{M}_0 \lesssim \min(M_\bullet^{\text{obs}}) \sim 10^6 M_\odot$ follows directly from basic local physics (tidal disruption and loss-cone dynamics) and empirical global properties of the Universe (its age and a universal M_\bullet/σ_* relation). Our derivation of \mathcal{M}_0 rests on four assumptions. (1) There is effective accretion of tidally disrupted stars (f_a is a few $\times 0.1$)²⁰. (2) Most black hole seeds were formed early, at a look-back time $t_i \sim \mathcal{O}(t_H)$. (3) Black hole growth is not typically mass or density limited; that is, the growing black hole is embedded in a stellar system with $M_{\text{sys}} \gg r_h^3 M_* n_* > M_\bullet$ for a substantial fraction of t_H . (4) The boundary conditions at r_h are set by the universal M_\bullet/σ_* relation at all times.

An early start for black hole seeds, and the requirement that a system that can form and retain a seed black hole

should be dense and massive enough, are both physically plausible and possibly even essential¹⁰. Such a system can be approximated as embedded in an isothermal density distribution, and is dynamically relaxed (see Methods section). Furthermore, the accretion rate of stars in a system with N_* stars inside r_h , $dM_\bullet/dt \simeq f_a M_* N_* / (\log(1/j_{lc}) T_R)$ (equation (16)), is slow enough to allow it to remain near equilibrium as it grows, as the timescale for growth by order of the stellar mass, $(dM_\bullet/dt)/(M_* N_*)$, is longer by a factor $\log(1/j_{lc})/f_a \gg 1$ than the timescale to return to steady-state, $T_{SS} \simeq T_R/4$ (ref. ²¹). The least secure assumption is that a universal M_\bullet/σ_* relation holds near its present-day value as the black hole grows. However, this is broadly consistent with observations of active galactic nuclei^{14,23} up to $z \sim 1$, and with simulations of large scale structure evolution^{24,25} up to $z \sim 4$.

Mergers between two central black holes increase the black hole mass, but also affect the dynamics around it. Mergers initially enhance the TDE rate²⁶, but later they may strongly suppress it by ejecting the cusp. However, steady-state is quickly re-established around IMBHs, $T_{SS}(M_\bullet \lesssim 10^5 M_\odot) < \mathcal{O}(10^8 \text{ yr})$ (ref. ²¹). Additional growth channels thus only increase present-day black hole masses, and reinforce the conclusion that central black holes with $M_\bullet < \mathcal{M}_0$ are rare.

Figure 2 shows the evolution of the lower mass limit \mathcal{M}_z , which increases rapidly with decreasing redshift to its present-day value \mathcal{M}_0 . Present-day IMBHs may exist in recently formed systems, in mass-limited ones (for example globular clusters with $M < 10^6 M_\odot$), in sub-galactic systems where the M_\bullet/σ_* relation need not apply (such as globular clusters or super star clusters), or in very low density galaxies (such as cored dwarfs²⁷). However, it is unlikely that such systems can form a black hole seed to start with^{1,10}, and therefore the black hole occupation fraction there is probably low. Candidate IMBHs have been reported in globular clusters and dwarf galaxies, including recently^{28,29}, but the evidence remains inconclusive.

Early TDE-driven growth and the suppression of the cosmic black hole mass function below \mathcal{M}_0 have implications for black hole seed evolution, for the cosmic rates and properties of TDEs⁸, and for gravitational waves (GWs) from IMBH-IMBH mergers and intermediate-mass-ratio inspirals into IMBHs. We conclude by listing these briefly.

A high rate of TDEs can allow black hole seeds to continue growing despite the ejection of the ambient gas by supernovae feedback³⁰. The lack of IMBHs at low redshifts means that electromagnetic searches will have to reach very deep to detect TDEs from IMBHs (jetted TDEs may provide an opportunity³¹). The prospects of detecting exotic processes related to IMBHs, such as tidal detonations of white dwarfs in the steep tidal field of a low-mass black hole³², will be low. The mean observed TDE rate per galaxy, $\Gamma \sim 10^{-5} \text{ yr}^{-1} \text{ gal}^{-1}$, is much lower than predicted rates³³. A dearth of black holes below \mathcal{M}_0 may partially resolve the rate discrepancy.

IMBHs produce GWs by intermediate-mass-ratio inspirals and by IMBH mergers. Detection of intermediate-mass-ratio inspirals by planned space-borne GW observatories^{9,34} is limited to redshifts below a few $\times 0.1$, and is therefore unlikely. However, IMBH mergers can be detected to very high redshifts. A GW search for IMBH mergers and intermediate-mass-ratio inspirals can reveal the formation history of black holes. We predict that black hole seeds are driven early on to higher mass by the ac-

cretion of stars, and therefore IMBHs are rare in the present-day Universe, but will be found near their high formation redshifts.

Methods

This supplement summarizes results from loss-cone theory used to derive the equation for black hole growth by stellar disruptions, and discusses the properties of its solutions. We first present, without derivation, a recipe for the approximate power-law growth rate equation (equation (1)), which has the advantage of leading to simple analytic results. We then comment on the general properties of its solutions, to clarify under what circumstances, and to what extent can simple dimensional analysis be used to estimate the minimal mass limit \mathcal{M}_0 . We then describe how the intrinsic scatter in the M_\bullet/σ_* relation is propagated through the growth equation to obtain the probability distributions for the lower limits \mathcal{M}_0 and \mathcal{S}_0 . Finally, we present for completeness and reproducibility an outline of the derivation of the full growth rate equation (used to verify our approximations, see Figure 1) and of its power-law approximation.

Approximate power-law black hole growth rate equation. We focus here on a steady-state stellar system around a black hole³⁵, which has a density cusp $n_* \propto r^{-\alpha}$ with $\alpha = 7/4$ inside the radius of influence $r_h = GM_\bullet/\sigma_*^2$. We further assume that the cusp is embedded in an external isothermal stellar distribution, $\rho(r) = \sigma_*^2/(2\pi Gr^2)$, so that the stellar mass enclosed inside r_h is twice the black hole mass¹⁸. Under the assumption of a universal M_\bullet/σ_* relation $M_\bullet = M_s(\sigma_*/\sigma_s)^\beta$, the dynamics leading to tidal disruption are characterized by a critical mass scale $M_c \sim 10^6 M_\odot$. Tidal disruptions are dominated by stars originating from $\sim r_h(M_\bullet)$ for $M_\bullet \geq M_c$, and by stars originating from an inner critical radius $r_c(M_\bullet) < r_h(M_\bullet)$ for $M_\bullet < M_c$ (see below for more details)³⁶. The TDE rate is well-approximated by a broken power-law (Figure 1)

$$\Gamma \simeq \Gamma_*(M_\bullet/M_*)^b, \quad (4)$$

whose index b changes across M_c , which is given by (see equations (20–21) for the general case),

$$M_c \simeq M_* \left(\frac{16}{5s^2} \right)^{3\beta/(6+\beta)}, \quad (5)$$

in terms of the dimensionless velocity dispersion scale $s = (M_s/M_*)^{-1/\beta} \sigma_s/v_*$, where $v_*^2 = GM_*/R_*$ and M_* and R_* are the mass and radius of a typical star in the system, and where we approximated the logarithmic term (equation (14)) appearing in the general expressions by a typical value $\Lambda_{lc} = 2$. The index b is (see equation (22) for the general case),

$$b = \begin{cases} (105 - 23\beta)/27\beta & M_\bullet \leq M_c \\ (3 - \beta)/\beta & M_\bullet > M_c \end{cases}. \quad (6)$$

Note that $b \ll 1$ for the empirically determined range of the M_\bullet/σ_* relation index^{3,13}, $4 \lesssim \beta < 6$. Defining $t_* = \sqrt{R_*^3/GM_*}$, the rate factor is

$$\Gamma_* \simeq \frac{5/4}{t_*} s^{40/9} \begin{cases} 1 & M_\bullet \leq M_c \\ (M_c/M_s)^{4(6+\beta)/27\beta} & M_\bullet > M_c \end{cases}. \quad (7)$$

To summarize, the approximate power-law TDE rate for a black hole with mass M_\bullet is calculated as follows. (1) Calculate the critical mass M_c (equation (5)). (2) Calculate the power-law index b (equation (6)) according to the low or high mass branch, depending on M_\bullet , and similarly calculate the rate factor Γ_* (equation (7)). (3) Use equation (4) to obtain the TDE rate from Γ_* and b .

Properties of the black hole growth solutions. The general solution of the growth equation (equation (4)) with the initial condition $M_\bullet(t=0) = M_i$ is

$$M_\bullet(t) = \begin{cases} M_\star[(M_i/M_\star)^{1-b} + (1-b)t/t_a]^{1/(1-b)} & b \neq 1 \\ M_i e^{t/t_a} & b = 1 \end{cases}, \quad (8)$$

where $t_a = (f_a \Gamma_\star)^{-1}$ is the accretion timescale. The growth solution has three branches. The solution for $b = 1$ diverges exponentially to infinity in infinite time. When $b > 1$, M_\bullet diverges on a finite timescale

$$t_\infty = t_a (M_i/M_\star)^{1-b} / |1-b|, \quad (9)$$

and is supra-exponential. The $b < 1$ branch is sub-exponential and diverges slowly as a power-law.

Exponential growth describes, for example, radiation pressure-regulated accretion of gas at the Eddington limit. Supra-exponential growth describes Hoyle-Lyttleton wind accretion³⁷, spherical Bondi accretion³⁸, or their generalization of accretion on an accelerating black hole³⁹. Sub-exponential growth, which is the relevant case for tidal accretion with the universal M_\bullet/σ_\star relation, at $t \gg t_\infty$ asymptotically approaches a power law that is independent of seed mass M_i

$$M_\bullet(t)/M_\star \simeq [(1-b)t/t_a]^{1/(1-b)}. \quad (10)$$

There are two mass scales in the growth equation: the initial mass M_i , and the natural mass scale^{40,41} M^{TDE} , obtained by solving $M^{\text{TDE}}/M_\star = f_a \Gamma t_H = f_a \Gamma_\star t_H (M^{\text{TDE}}/M_\star)^b$ with $t_H = 10^{10}$ yr. This mass scale was used in past studies^{17,18,33} to estimate $M_\bullet(t_H)$. It is instructive to analyze the role of M^{TDE} in the growth solutions, and identify when it can provide a relevant estimate for the black hole mass.

The exponential and supra-exponential solutions ($b \geq 1$) are functions of M_i on all timescales, and M_\bullet^{TDE} plays there a role related to the exponential or divergence timescales. Because these solutions diverge, the black hole mass at any finite time is generally unrelated to either M_i or M_\bullet^{TDE} . The asymptotic sub-exponential solution ($b < 1$) can be written as $M_\bullet(t_H) = M_\bullet^{\text{TDE}}(1-b)^{1/(1-b)}$. In this case, M_\bullet^{TDE} provides a reasonable approximation for M_\bullet as long as $|b| \ll 1$. This is the indeed case for the empirical universal M_\bullet/σ_\star relation, where $b(\alpha = 7/4, \beta = 5.40) \simeq -0.125$. However, other combinations of cusp and M_\bullet/σ_\star indices can lead to arbitrarily large disparities: for example $b(\alpha = 3/2, \beta = 3) \simeq 0.6$, results in $M_\bullet \simeq 0.1 M_\bullet^{\text{TDE}}$.

It should be emphasized that the solution branch that describes the black hole growth is not determined solely by the assumed growth channel — tidal disruptions in this case — but also by the choice of boundary conditions, which here are determined by an empirical relation. Other possible values of cusp and M_\bullet/σ_\star indices would imply very different relations between M_\bullet and M_\bullet^{TDE} . For example, the transition to the exponential and supra-exponential solutions ($b \geq 1$) occurs for $\beta \leq 2.1$ (for $\alpha = 7/4$) or for $\beta \leq 3$ (for $\alpha = 1/2$). Therefore, it is not generally true that M_\bullet^{TDE} estimates the black hole mass. Its relevance depends on the specific solution and on the adopted boundary conditions, and cannot be assumed a priori.

Intrinsic M_\bullet/σ_\star scatter and distribution of lower limits. The observed intrinsic scatter in the M_\bullet/σ_\star relation at $z \simeq 0$, with r.m.s δ_ϵ , can be interpreted as reflecting a variance in the initial conditions of individual galaxies at their formation, a Hubble time t_H ago, or a variance that developed gradually over their individual evolutionary histories and reached the observed rms value at t_H .

We assume that the estimation errors in the parameters α and β of the M_\bullet/σ_\star relation, $\log(M_\bullet/M_\star) = (\bar{\alpha} \pm \delta_\alpha) + (\bar{\beta} \pm \delta_\beta) \log(\sigma/\sigma_s) \pm \delta_\epsilon$, can be approximated by a correlated bi-Gaussian distribution, $(\alpha, \beta) \sim G_2(\bar{\alpha}, \delta_\alpha, \bar{\beta}, \delta_\beta, \rho_{\alpha\beta})$, where for an arbitrarily chosen low reference velocity dispersion $\sigma_s \ll \sigma$, the correlation coefficient

$\rho_{\alpha\beta} \rightarrow -1$ (ref. ⁴²), and that the intrinsic scatter ϵ is drawn from a Gaussian distribution, $\epsilon \sim G(0, \delta_\epsilon)$.

We approximate the evolution of the scatter by assuming n_t discrete time steps of duration $\Delta t = t_H/n_t$, where the accumulated change in α due to scatter, $\Delta\epsilon$, is modified in a random walk fashion by $\Delta\epsilon \rightarrow \Delta\epsilon + \epsilon/\sqrt{n_t}$. We then evolve the black hole mass over time Δt by the growth equation (equation (8)), and repeat until $t = t_H$. The joint and marginal probability distributions for \mathcal{M}_0 and \mathcal{S}_0 at t_H are obtained by Monte Carlo simulations over randomly drawn values of α and β .

The limit $n_t = 1$ corresponds to scatter that is determined by the galaxy's initial conditions, whereas $n_t \gg 1$ corresponds to scatter that is determined by the galaxy's evolution. We find that the probability distributions for \mathcal{M}_0 and \mathcal{S}_0 do not depend strongly on the choice of n_t , and that they converge rapidly for $n_t > 3$ to an asymptotic form. The values quoted in this study, 5% lower limits of $\mathcal{M}_0 = 2.8 \times 10^5 M_\odot$ and $\mathcal{S}_0 = 38 \text{ km s}^{-1}$, correspond to the asymptotic evolutionary scatter case ($n_t = 5$), whereas the initial scatter case ($n_t = 1$) differs only slightly, with 5% lower limits of $\mathcal{M}_0 = 1.9 \times 10^5 M_\odot$ and $\mathcal{S}_0 = 36 \text{ km s}^{-1}$.

Full black hole growth rate equation. The tidal disruption (plunge) rate can be approximated by the flux of stars into the black hole from the boundary between the inner region, where stars slowly diffuse into the loss-cone (the empty loss-cone) and the outer region, where stellar scattering is strong enough that the loss-cone is effectively full (the full loss-cone)³⁶. The boundary is at a critical radius, a_c , that satisfies

$$q = \frac{[J_c(a_c)/J_{lc}]^2 P(a_c)}{\log(J_c(a_c)/J_{lc}) T_R(a_c)} = 1, \quad (11)$$

where $P = 2\pi \sqrt{a^3/GM_\bullet}$ is the orbital period, $J_c = \sqrt{GM_\bullet a}$ is the circular angular momentum at a , J_{lc} is angular momentum of the loss-cone ($J_{lc} \simeq \sqrt{2GM_\bullet} Q^{1/3} R_\star$ for tidal disruption, so $J_c/J_{lc} \simeq \sqrt{(a/R_\star)/2Q^{1/3}}$, where $Q = M_\bullet/M_\star$). T_R is the 2-body (non-resonant) relaxation time²¹,

$$T_R(a) = \frac{5}{8} \frac{Q^2 P(a)}{N_\star(a) \log(Q)}, \quad (12)$$

where $N_\star(a) = \mu_h Q(a/r_h)^{3-\alpha}$ is the number of stars enclosed in r , and $r_h = \eta_h GM_\bullet/\sigma_\star^2$ is the radius of influence. The numeric prefactors are conventionally assumed to be $\mu_h = 2$ and $\eta_h = 1$. We further assume that $\alpha < 9/4$.

The exact solution for the critical radius can be written by the implicit equation

$$\begin{aligned} a_c/r_h &= (A_c \sigma_\star^2/v_\star^2)^{1/(4-\alpha)} Q^{1/(12-3\alpha)} \\ &= (A_c s^2)^{1/(4-\alpha)} Q^{(\beta+6)/\beta(12-3\alpha)}, \end{aligned} \quad (13)$$

where $A_c = 5/(4\mu_h \Lambda_{lc} \eta_h)$ and

$$\Lambda_{lc}(Q, a) = \log Q / \log(J_c(a)/J_{lc}), \quad (14)$$

where the last equality in equation (13) assumes the M_\bullet/σ_\star relation in terms of the dimensionless velocity dispersion scale $s = (M_s/M_\star)^{-1/\beta} \sigma_s/v_\star$, where $v_\star = \sqrt{GM_\star/R_\star}$.

When $a_c > r_h$, the rate is estimated⁴³ at r_h . The transition occurs above a critical black hole mass such that $a_c(M_c) = r_h(M_c)$,

$$M_c = M_\star (A_c \sigma_\star^2/v_\star^2)^{-3} = M_\star (A_c s^2)^{-3\beta/(6+\beta)}, \quad (15)$$

which is independent of α and almost independent of β . The plunge rate can then be conservatively approximated by the empty loss-cone rate at $a_e = \min(a_c, r_h)$,

$$\Gamma \simeq \frac{N_\star(a_e)}{\log(J_c(a_e)/J_{lc}) T_R(a_e)} = \frac{8 \Lambda_{lc} \mu_h^2}{5 P(r_h)} \left(\frac{a_e}{r_h} \right)^{(9-4\alpha)/2}. \quad (16)$$

The actual rate, including the contribution from the full loss-cone regime, can be up to twice as high as this⁴³.

Using $r_h = \eta_h GM_\bullet / \sigma_\star^2$, the plunge rate can be represented as

$$\Gamma^\Lambda = \frac{1}{\pi t_\star} \begin{cases} \gamma_c^\Lambda Q^{(2\alpha-15)/6(4-\alpha)} \left(\frac{\sigma_\star}{v_\star}\right)^{7(3-\alpha)/(4-\alpha)} & M_\bullet \leq M_c \\ \gamma_h^\Lambda Q^{-1} \left(\frac{\sigma_\star}{v_\star}\right)^3 & M_\bullet > M_c \end{cases}, \quad (17)$$

where $t_\star = \sqrt{R_\star^3/GM_\star}$,

$$\gamma_c^\Lambda = \left(\frac{4\Lambda_{lc}}{5}\right)^{(2\alpha-1)/(8-2\alpha)} \left(\frac{\mu_h}{\eta_h^{(3-\alpha)}}\right)^{7/(8-2\alpha)}, \quad (18)$$

and

$$\gamma_h^\Lambda = \frac{4\mu_h^2 \Lambda_{lc}}{5\eta_h^{3/2}}. \quad (19)$$

When σ_\star is given by the M_\bullet/σ_\star relation, the rate can be expressed as

$$\Gamma = \Gamma_\star^\Lambda Q^b, \quad (20)$$

where

$$\Gamma_\star^\Lambda = \frac{\gamma_c^\Lambda}{\pi t_\star} s^{7(3-\alpha)/(4-\alpha)} \begin{cases} 1 & M_\bullet \leq M_c \\ \left(\frac{M_c}{M_\bullet}\right)^{(6+\beta)(9-4\alpha)/6(4-\alpha)\beta} & M_\bullet > M_c \end{cases}. \quad (21)$$

The notation Γ_\star^Λ denotes the weak functional dependence on Q via the logarithmic term $\Lambda_{lc} \simeq 2$. The index is

$$b = \begin{cases} 7(3-\alpha)/\beta(4-\alpha) - (15/2 - \alpha)/3(4-\alpha) & a_c \leq r_h \\ (3-\beta)/\beta & a_c > r_h \end{cases}. \quad (22)$$

A simpler power-law approximation can be obtained by choosing this typical value for the logarithmic term $\Lambda_{lc} \simeq 2$. Then, $\Gamma \simeq \Gamma_\star^\Lambda Q^b$ (see above), where the normalization $\Gamma_\star = \Gamma_\star^\Lambda(\Lambda_{lc} = 2)$ is not a function of Q .

Figure 1 shows the TDE rates for $\mu_h = 2$, $\eta_h = 1$ in the two dynamical regimes $a_c < r_h$ and $a_c > r_h$ ($Q < Q_c$ and $Q > Q_c$). At the lower mass end, the mean mass accretion rate may rise above the Eddington rate. For example, for $\beta = 5$, $L_{TD}/L_E \lesssim 6$ at $M_\bullet = 10^3 M_\odot$, but falls below $L_{TD}/L_E = 1$ for $M_\bullet > 5 \times 10^3 M_\odot$. Depending on the exact value of the logarithmic slope of the M_\bullet/σ_\star relation, β , the TDE rate on the low-mass branch, can either rise or fall with M_\bullet .

Data availability statement The numeric results that support the plots within this paper and other findings of this study are available from the corresponding author upon reasonable request.

Acknowledgements We are grateful for helpful discussions with Y. Alexander, J. Gair, A. Gal-Yam, J. Green, J. Guillochon, M. MacLeod, N. Neumayer, T. Piran, E. Rossi, A. Sesana, J. Silk, N. Stone and B. Trakhtenbrot. TA acknowledges support by the I-CORE Program of the Planning and Budgeting Committee and The Israel Science Foundation (grant No 1829/12). BB acknowledges support by NASA (grant NNX14AM24G) and by the NSF (grant AST-1406166).

Author Contributions TA and BB developed the ideas presented in this paper together and collaborated in its writing.

Correspondence Correspondence and requests for materials should be addressed to Tal Alexander (tal.alexander@weizmann.ac.il) or Ben Bar-Or (benbaror@ias.edu).

Competing Interests The authors declare that they have no competing financial interests.

1. Miller, M. C. & Colbert, E. J. M. Intermediate-Mass Black Holes. *International Journal of Modern Physics D* **13**, 1–64 (2004).
2. Abbott, B. P. *et al.* Observation of gravitational waves from a binary black hole merger. *Phys. Rev. Lett.* **116**, 061102 (2016).
3. Graham, A. W. Galaxy Bulges and Their Massive Black Holes: A Review. In Laurikainen, E., Peletier, R. & Gadotti, D. (eds.) *Galaxy Bulges*, vol. 418 of *Astrophysics and Space Science Library*, 263–313 (Springer International Publishing Switzerland, 2016).
4. Ferrarese, L. & Merritt, D. A Fundamental Relation between Supermassive Black Holes and Their Host Galaxies. *Astrophys. J.* **539**, L9–L12 (2000).
5. Gebhardt, K. *et al.* A Relationship between Nuclear Black Hole Mass and Galaxy Velocity Dispersion. *Astrophys. J.* **539**, L13–L16 (2000).
6. McConnell, N. J. & Ma, C.-P. Revisiting the Scaling Relations of Black Hole Masses and Host Galaxy Properties. *Astrophys. J.* **764**, 184 (2013).
7. van den Bosch, R. C. E. Unification of the fundamental plane and Super Massive Black Hole Masses. *Astrophys. J.* **831**, 134 (2016).
8. Rees, M. J. Tidal disruption of stars by black holes of 10 to the 6th–10 to the 8th solar masses in nearby galaxies. *Nature* **333**, 523–528 (1988).
9. Amaro-Seoane, P. *et al.* eLISA: Astrophysics and cosmology in the millihertz regime. *GW Notes*, Vol. 6, p. 4–110 **6**, 4–110 (2013).
10. Volonteri, M. The Formation and Evolution of Massive Black Holes. *Science* **337**, 544 (2012).
11. Mortlock, D. J. *et al.* A luminous quasar at a redshift of $z = 7.085$. *Nature* **474**, 616–619 (2011).
12. Bennett, C. L., Larson, D., Weiland, J. L. & Hinshaw, G. The 1% Concordance Hubble Constant. *Astrophys. J.* **794**, 135 (2014).
13. Kormendy, J. & Ho, L. C. Coevolution (Or Not) of Supermassive Black Holes and Host Galaxies. *Ann. Rev. Astron. Astrophys.* **51**, 511–653 (2013).
14. Shen, Y. *et al.* The Sloan Digital Sky Survey Reverberation Mapping Project: No Evidence for Evolution in the $M_\bullet - \sigma_\star$ Relation to $z \sim 1$. *Astrophys. J.* **805**, 96 (2015).
15. Alexander, T. Key Questions about Galactic Center Dynamics. In Morris, M. R., Wang, Q. D. & Yuan, F. (eds.) *The Galactic Center: a Window to the Nuclear Environment of Disk Galaxies*, vol. 439 of *ASP Conf. Ser.*, 129 (2011).
16. Bar-Or, B. & Alexander, T. Steady-state Relativistic Stellar Dynamics Around a Massive Black hole. *Astrophys. J.* **820**, 129 (2016).
17. Magorrian, J. & Tremaine, S. Rates of tidal disruption of stars by massive central black holes. *Mon. Not. R. Astron. Soc.* **309**, 447–460 (1999).
18. Merritt, D. *Dynamics and Evolution of Galactic Nuclei* (Princeton: Princeton University Press, 2013).
19. Stone, N. C., Küpper, A. H. W. & Ostriker, J. P. Formation of massive black holes in galactic nuclei: runaway tidal encounters. *Mon. Not. R. Astron. Soc.* **467**, 4180–4199 (2017). 1606.01909.
20. Ayal, S., Livio, M. & Piran, T. Tidal Disruption of a Solar-Type Star by a Supermassive Black Hole. *Astrophys. J.* **545**, 772–780 (2000).
21. Bar-Or, B., Kupi, G. & Alexander, T. Stellar Energy Relaxation around a Massive Black Hole. *Astrophys. J.* **764**, 52 (2013).
22. Xiao, T. *et al.* Exploring the Low-mass End of the $M_{BH} - \sigma_\star$ Relation with Active Galaxies. *Astrophys. J.* **739**, 28 (2011).
23. Salviander, S. & Shields, G. A. The Black Hole Mass-Stellar Velocity Dispersion Relationship for Quasars in the Sloan Digital Sky Survey Data Release 7. *Astrophys. J.* **764**, 80 (2013).
24. Sijacki, D. *et al.* The Illustris simulation: the evolving population of black holes across cosmic time. *Mon. Not. R. Astron. Soc.* **452**, 575–596 (2015).
25. Taylor, P. & Kobayashi, C. Time evolution of galaxy scaling relations in cosmological simulations. *Mon. Not. R. Astron. Soc.* **463**, 2465–2479 (2016).
26. Chen, X., Sesana, A., Madau, P. & Liu, F. K. Tidal Stellar Disruptions by Massive Black Hole Pairs. II. Decaying Binaries. *Astrophys. J.* **729**, 13 (2011).
27. Walker, M. G. *et al.* A Universal Mass Profile for Dwarf Spheroidal Galaxies? *Astrophys. J.* **704**, 1274–1287 (2009).
28. Baldassare, V. F., Reines, A. E., Gallo, E. & Greene, J. E. A $\sim 50,000 M_\odot$ Solar Mass Black Hole in the Nucleus of RGG 118. *Astrophys. J.* **809**, L14 (2015).
29. Kızıltan, B., Baumgardt, H. & Loeb, A. An intermediate-mass black hole in the centre of the globular cluster 47 Tucanae. *Nature* **542**, 203–205 (2017).

30. Dubois, Y. *et al.* Black hole evolution - I. Supernova-regulated black hole growth. *Mon. Not. R. Astron. Soc.* **452**, 1502–1518 (2015).
31. Fialkov, A. & Loeb, A. Jetted Tidal Disruptions of Stars as a Flag of Intermediate Mass Black Holes at High Redshifts. *ArXiv e-prints* (2016). 1611.01386.
32. Rosswog, S., Ramirez-Ruiz, E. & Hix, W. R. Tidal Disruption and Ignition of White Dwarfs by Moderately Massive Black Holes. *Astrophys. J.* **695**, 404–419 (2009).
33. Stone, N. C. & Metzger, B. D. Rates of stellar tidal disruption as probes of the supermassive black hole mass function. *Mon. Not. R. Astron. Soc.* **455**, 859–883 (2016).
34. Yagi, K. Scientific Potential of Decigo Pathfinder and Testing GR with Space-Borne Gravitational Wave Interferometers. *International Journal of Modern Physics D* **22**, 1341013 (2013).
35. Bahcall, J. N. & Wolf, R. A. Star distribution around a massive black hole in a globular cluster. *Astrophys. J.* **209**, 214–232 (1976).
36. Lightman, A. P. & Shapiro, S. L. The distribution and consumption rate of stars around a massive, collapsed object. *Astrophys. J.* **211**, 244–262 (1977).
37. Hoyle, F. & Lyttleton, R. A. The effect of interstellar matter on climatic variation. *Proceedings of the Cambridge Philosophical Society* **35**, 405 (1939).
38. Bondi, H. On spherically symmetrical accretion. *Mon. Not. R. Astron. Soc.* **112**, 195–+ (1952).
39. Alexander, T. & Natarajan, P. Rapid growth of seed black holes in the early universe by supra-exponential accretion. *Science* **345**, 1330–1333 (2014). 1408.1718.
40. Murphy, B. W., Cohn, H. N. & Durisen, R. H. Dynamical and luminosity evolution of active galactic nuclei - Models with a mass spectrum. *Astrophys. J.* **370**, 60–77 (1991).
41. Freitag, M. & Benz, W. A new Monte Carlo code for star cluster simulations. II. Central black hole and stellar collisions. *Astron. Astrophys.* **394**, 345–374 (2002).
42. Tremaine, S. *et al.* The Slope of the Black Hole Mass versus Velocity Dispersion Correlation. *Astrophys. J.* **574**, 740–753 (2002).
43. Syer, D. & Ulmer, A. Tidal disruption rates of stars in observed galaxies. *Mon. Not. R. Astron. Soc.* **306**, 35–42 (1999).